Renewable and Sustainable Energy Reviews 41 (2015) 915–931

Contents lists available at ScienceDirect

Renewable and Sustainable Energy Reviews

journal homepage: www.elsevier.com/locate/rser

# Modelling solar potential in the urban environment: State-of-the-art review

S. Freitas *, C. Catita, P. Redweik, M.C. Brito

*Instituto Dom Luiz, Faculdade de Ciências, Universidade de Lisboa, 1749-016 Lisboa, Portugal*

ARTICLE INFO

*Article history:*
Received 22 February 2014
Received in revised form
17 July 2014
Accepted 22 August 2014

*Keywords:*
Solar potential
GIS
Urban model
Solar mapping
Photovoltaic

ABSTRACT

Cityscapes provide a complex environment, where solar radiation is unevenly distributed, especially since urban features started to propagate more and more vertically. Due to the dynamic overshadowing effects present on building surfaces, quantifying these phenomena is essential for predicting reductions in solar radiation availability that can significantly affect potential for solar energy use. Numerical radiation algorithms coupled with GIS tools are a pathway to evaluate those complex effects. Accurate representation of the terrain, vegetation canopy and building structures allows better estimation of shadow patterns. Higher spatial and temporal resolutions deliver more detailed results, but models must compromise between accuracy and computation time. In this paper, models ranging from simple 2D visualization and solar constant methods, to more sophisticated 3D representation and analysis, are reviewed. Web-based solar maps, which rely on the previous features to successfully communicate the benefits of the solar resource to the public and support in the policy-making process, are also addressed.

© 2014 Elsevier Ltd. All rights reserved.

**Contents**



* Correspondence to: Centre for Sustainable Energy Systems of the University of Lisbon (SESUL), Campo Grande, Ed. C8 (8.3.33), 1749-016 Lisboa, Portugal. Tel.: +351 962 497 716.
*E-mail address:* srefreitas@fc.ul.pt (S. Freitas).

http://dx.doi.org/10.1016/j.rser.2014.08.060
1364-0321/© 2014 Elsevier Ltd. All rights reserved.

## 1. Introduction

Solar radiation is a clean and abundant source of energy. With fast technological improvement, decreasing costs and increasing public acceptance, solar energy will surely play a relevant share of future energy systems. Since a significant fraction of energy is consumed in cities, the deployment of photovoltaics (PV) and solar thermal (ST) collectors in the urban environment is gaining increasing interest. Thanks to their high modularity, ST and PV systems are slowly driving the decentralization of electricity and heat production, which is a cornerstone of the Nearly Zero Energy Buildings (nZEB) concept, where buildings become almost independent from the electrical grid due to a thorough integration of renewable energy sources and building designs, maximizing natural ventilation, daylighting, etc. [1].

Urban structures, however, are not always suitable for solar energy applications. While in non-urban environment the constraints to energy yields are mostly related to unfavourable meteorological conditions, in urban environments the limited available area and obstructions to the incoming sunlight also limits the attainment of full solar potential. Thus, before the deployment of an urban solar power plant, it is essential to model the local solar resource in order to evaluate the feasibility of the system. Depending on the end-goal and the level of detail required, some methodologies will be more appropriate than others. For instance, a straightforward solar potential estimate by simple and generalist methods is a standard practice for small scale rooftop installations. On the other hand, a complete urban environment analysis must account for intricate shadowing events, which calls for more complex approaches to achieve higher reliability, particularly when vertical surfaces such as building facades are included.

Izquierdo et al. [2] identifies a hierarchical approach when studying the use of a specific renewable resource such as the solar radiation, introducing gradual restrictions to define different levels of potential. The first one is the physical potential, which encompasses the maximum amount of solar energy that can be received in a certain area. Then, the geographic potential is calculated by gradually excluding the zones reserved for other uses, restricting the locations where solar energy can be gathered. Finally, the technical potential takes into account the technical characteristics of the equipment used for the conversion of electrical energy. An economic potential and a social potential can also be addressed to deal with the deployment prospects.

Earlier solar potential tools enabled the computation of the physical potential in non-urban scenarios, individual rooftops or 2D building-like geometries [3–6]. Today, thanks to great improvement in computer power and modelling techniques, solar geographical and technical potential in the cityscape can be estimated, analysed and represented at a small scale using Computer-Aided Design (CAD) software [7,8] and at a macroscale via geographical information system (GIS) tools [9–12], which are able to manipulate large amounts of geo-referenced data. Nevertheless, it has to be highlighted that, contrarily to 2D approaches for which the procedure is relatively straightforward and GIS tools are completely able to perform any kind of spatial analysis, the computation of solar radiation at specific points of a 3D arrangement is still a challenge for GIS. In some cases, the computation of solar radiation is first performed by numerical computation software and only then introduced into the GIS.

The more levels of potential a model is able to perform, the easier it is to successively communicate the advantages of building integrated solar systems to the general public. More than promoting solar energy for ST and PV end-users, it is possible to help policy-making processes, for instance, by studying all available energy resources of a country [13] or defining the most interesting areas in a city. In this context, the outcomes may support the implementation of energy measures or establish a long-term energy supply and demand strategy. Koo et al. [14] presents an example of a framework involving solar resource assessment and GIS to support government policy.

## 2. General methodology

To perform a detailed estimation of the physical and geographic solar potential, a series of steps must be taken. Fig. 1 summarizes this sequential approach. A set of information regarding the relevant features of the surfaces and their surroundings is required, i.e. a Digital Surface Model (DEM), whenever the scale and the context of the analysis requires such detail. This type of data can be obtained through the means of several techniques, such as simple aerial or satellite imagery, Light Detection and Ranging (LiDAR) that stores the geometrical information of a scanned surface as a 3D point cloud, stereo imagery which consists of pairs of geo-referenced photographic images covering the city and allowing to create a 3D model of the city by photogrammetry. Available cadastre data can also be employed to generate a 3D city model but this is more common in 2D applications, such as using building footprints for simple rooftop solar potential evaluation.

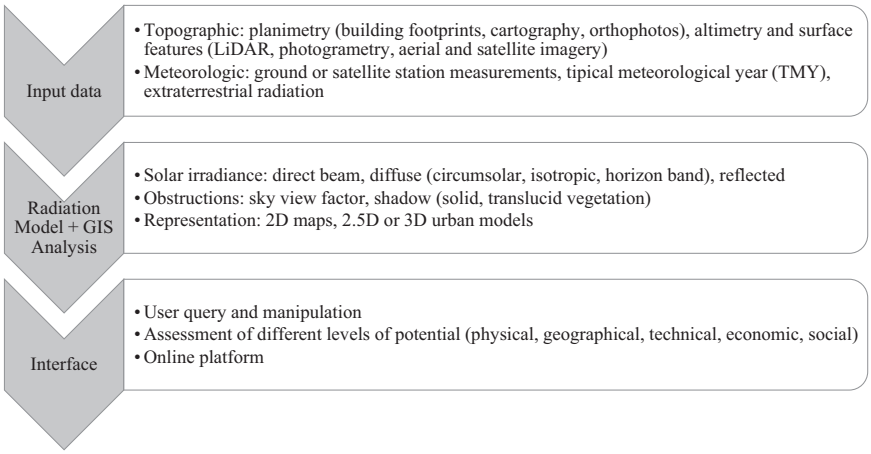


**Fig. 1.** Steps and options involved in the assessment of solar potential at a certain location.

Secondly, a generic solar radiation model or a local model obtained from climatic observations is needed for the algorithm to be completed. Whether collected from ground-based meteorological stations or derived from satellites, climate measurements allow the computation of irradiance at any tilt making use of some geometric approaches to determine the position of the sun.

While in non-urban contexts the procedure is quite simple, the order of complexity rises when estimating the solar resource in cityscapes as it relates to tri-dimensional phenomena. Solar radiation is time, location and conditions dependent and the consequent shadows cast on surfaces by buildings, vegetation or structural elements make an obstruction analysis necessary.

Due to the wide range of concepts and approaches provided by the existing solar potential models, this document is structured in crescent model complexity, and somehow chronologically, with only physical and geographical potential in mind. Technical potential of ST or PV systems is out of the scope of this review.

In order to provide a layer of context, a brief look up on empirical solar models is first taken, in Section 3, and a chronological overview on the concepts and numerical tools developed for solar resource assessment is presented in the beginning of Section 4. Then, some of the most refined computational tools capable of handling 3D representations, and thus more urban-oriented, are explored. Finally, some relevant solar maps are also reviewed at the end of this section. Current limitations to the surveyed models are also discussed, together with emerging future trends.

## 3. Empirical solar radiation models

Meteorological stations generally measure global and diffuse irradiation received on the horizontal plane and the direct component can be obtained from:

$$G_{horiz} = Dir_{horiz} + Dif_{horiz} = Dir_{norm} \cos Z + Dif_{horiz} \quad (1)$$

where $G_{horiz}$ is the global horizontal irradiance, $Dir_{norm}$ is the direct normal irradiance, $Dif_{horiz}$ is the diffuse horizontal irradiance and $Z$ is the sun's zenith angle.

Using data series from ground stations implies that the irradiance that reaches other tilted surfaces has to be estimated. There are several geometrically-based formulations suited either to clear sky conditions or to overcast conditions taking cloud cover into account [15].

The classic methodology to determine global irradiance on a tilted surface, $G_{tilted}$, relies on previous knowledge of its components and can be evaluated through the following expression:

$$G_{tilted} = Dif_{horiz} F_{dif} + \rho G_{horiz} F_{ref} + Dir_{norm} \cos \theta \quad (2)$$

where $F_{dif}$ and $F_{ref}$ are, respectively, the transposition factors for diffuse and ground reflection, $\rho$ is the foreground's albedo and $\theta$ is the angle of incidence of the sun rays on the tilted plane. This angle can be evaluated by the trigonometric relation [16]:

$$\cos\theta = \cos\delta \sin\beta \sin\gamma \sin\omega + (\cos\varphi \cos\beta + \sin\varphi \sin\beta \cos\gamma) \times \cos\delta \cos\omega + (\sin\varphi \cos\beta - \cos\varphi \sin\beta \cos\gamma) \sin\delta \quad (3)$$

where $\delta$ is the declination angle, $\gamma$ is the latitude of the location, $\beta$ is the surface tilt, $\omega$ is the hour angle and $\varphi$ is the surface azimuth.

If the transposition of the direct component is rather simple, the scenario is not so straightforward for diffuse and ground-reflected radiation, as can be observed in Fig. 2, which features the two great unknowns in (2), $F_{dif}$ and $F_{ref}$. Assuming isotropy (4), (5), which means that the incoming diffuse radiation is the same from every direction, the approximation would be:

$$F_{dif} = \frac{1 + \cos\beta}{2} \quad (4)$$

$$F_{ref} = \frac{1 - \cos\beta}{2} \quad (5)$$

If the diffusion process is considered anisotropic, with different contributions according to the direction and environment features, the transposition factors have to be redefined. In this context, a level of specularity can also be defined, i.e. how preferentially the radiation propagates along a certain direction, and this depends on the characteristics of the surface material.

Surfaces, mainly south-facing when in the northern hemisphere, may also receive more diffuse radiation from the so-called circumsolar component, which refers to light that, to an observer on the ground, appears to originate from the region around the sun. This component is highly dependent on the percentage of haze, but can also vary when the solar disc reaches an obstacle to the sunlight at a certain point.

### 3.1. Transposition models

The simplest model considers diffuse radiation to be in the entire sky view [18] and that the global solar radiation has three components: direct beam, isotropic diffuse and diffusely reflected from the ground. More realistic models consider anisotropic diffuse irradiation, such as the Hay model [19] that assumes linearity of the isotropic and circumsolar contributions to the diffuse radiation on a tilted plane, defining an anisotropy index.

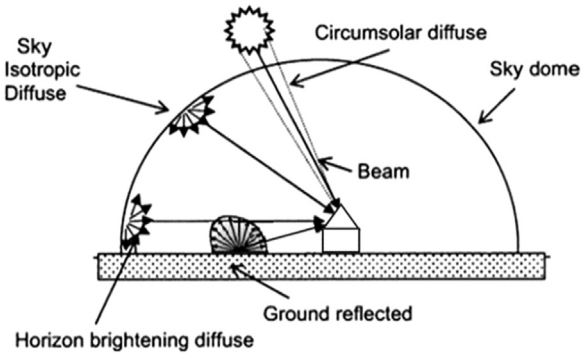


**Fig. 2.** Schematic representation of the radiation reaching a tilted surface by the sky anisotropic concept, including the anisotropy of the ground reflected component. It is important to note that the sky and horizon diffuse components may not be perfectly isotropic. Adapted from [17].

Perez et al. [20] incorporates a geometric description of the sky hemisphere superimposing a circumsolar disc and horizon band on an isotropic background. A parametric representation of solar irradiation is obtained through the use of multiple coefficients obtained from statistical regression analysis. This configuration accounts for forward scattering by aerosols and multiple Rayleigh scattering and retro-scattering near the horizon, two consistent anisotropic effects in the atmosphere.

The reflected component of radiation may also represent a source of uncertainty. The two quoted methods consider this contribution differently. The first considers multi-reflection from adjacent Lambertian surfaces whereas the second accounts for changes in ground albedo. However, reflected radiation is originated from the ground and also from vertical surroundings as an intricate 3D and again anisotropic phenomenon.

Choosing the proper radiation model for a certain application is not trivial and there is much diversity among models in literature. For instance, a comparison of 12 models for estimating total solar radiation on south and west facing tilted surfaces was performed in [21] were both original and simplified Perez [22,23] and Hay [19] models compared well to data from pyranometers. Mondol et al. [24] test the effect of 12 different combinations of diffuse–global correlations and tilted surface radiation models, concluding that Perez performs best in comparison to other anisotropic models, but prediction of PV performance was better with isotropic models. Evseev and Kudish [25] compare the ability of several models to predict the global solar radiation on a south-oriented surface tilted at 40° as a function of four different types of sky conditions. Here, Ma–Iqbal model [26] performs best under all sky, clear and partially cloudy conditions, whereas the Muneer [27] model gives the best results for cloudy sky. Gueymard in [28] takes 10 transposition models, either for optimal or suboptimal input data, against global radiation measured on south-facing planes at 40°, vertical and on a 2-axis tracker. It was found that for suboptimal input, Hay [19], Reindl [29] and Skartveit [30] models deliver better outputs. When ideal input and conditions are considered the results from anisotropic models are within the instrumental uncertainty, with Gueymard [31] and Perez [23] models performing best. On the other hand, for ideal input and all-sky conditions it was Reindl [29] which performs the best and gives noteworthy results for vertical surfaces, which are very sensitive to any inaccuracies in the ground reflected radiation due to its anisotropic features.

A methodology to calculate the global horizontal real sky irradiance was introduced by Grigiante et al. [32] by improving an existing model, the predictive Bird's clear sky model [33], through the introduction of atmospheric parameters such as the cloud cover factor, specifically defined for the location. The definition of *octas* sky covered conditions is proposed as an empirical evaluation of the sky brightness based on experimental data. A comparison with global radiometer measurements shows that the model, applied to a case study in a mountainous area, overestimated the reference data with an accuracy of 2.16%. This is, in fact, a fine result, but an approach on the global radiation incident on vertical surfaces would also be desirable.

In summary, Perez model is widely used and cited among the best performing models, and it has even been applied as a proxy radiation method from geostationary satellites in a modified version of the program PVFORM, to predict load match between generation and requirements of 20 utilities in the US [34]. For a comparison assessment of some of these diffuse radiation models and others see [35].

Recently, a detailed analytical approach to estimate diffuse radiation in obstructed environments was discussed in Ivanova [36,37], where vertical and horizontal surfaces are addressed for both overcast and non-overcast conditions. Anisotropic sky is taken into consideration highlighting that the introduction of certain diffuse radiation components, such as the horizon brightening diffuse, may not be appropriate in an urban context.

## 4. Computational solar radiation models

For real topographies, physically-based solar radiation formulations alone cannot compute radiation with obstructions to sunlight. Such analysis, for a large range of spatial and temporal scales, can only be performed with computational modelling of the physical context. It is relatively straightforward to model barriers to the direct radiation component but the reduction of diffuse irradiance from different sky directions is a major challenge, not only due to anisotropy but also due to the amount of visible sky at any given point.

### 4.1. Concepts and numerical methods

The following list includes most of the concepts and numerical methods found in literature. The most relevant characteristics of available computational solar models are outlined, along with their advantages and limitations. Some models feature concepts that are more suited to non-urban studies or less detailed assessments, due to their inability to model cityscape topographies, while others can handle complex 3D representation at a small scale. Table 1 summarizes their most relevant characteristics.

#### 4.1.1. GOSOL

One of the first simulation software [3], based on a model of a whole housing scheme, it can analyse energy balance on particular surfaces. Shading patterns can be visualized and it also produces an outline of obstructions on a sunpath diagram, graphically indicating the times of day and year when the sun can shine on a point in a layout. GOSOL includes vegetation and climate characteristics and centres the calculation on building data source of German housing types with restricted energy consumption, such as passive buildings.

#### 4.1.2. SHADOWPACK

Created by Peckham [4], SHADOWPACK uses its own CAD-type program developed to facilitate modest shading evaluations, for the direct component of solar radiation received by surfaces, which can be plotted as contour maps. View of the site can also be generated with the shadows at any particular time of day and year.

**Table 1**
Most relevant characteristics of the concepts and numerical solar radiation methods.

| Tool | Main purpose | Related solar potential | Starting year | References |
|---|---|---|---|---|
| GOSOL | Energy balance on particular surfaces using building data source of German housing types | Physical/ geographical | 1991 | [3] |
| SHADOWPACK | Contour maps of shading evaluations for the direct radiation | Physical | 1990 | [4] |
| ATM | Image processing framework can generate topoclimatologies for large areas at arbitrary time intervals | Geographical | 1992 | [38,39] |
| Sky view factor | Percentage of visible sky for diffuse radiation calculation | Physical/ geographical | 1987 | [39–44] |
| Solei-32 | Potential energy income to slopes with different orientations and cloudiness, shadow from surrounding topography | Geographical | 1993 | [46] |
| SolarFlux | Topographic GIS capabilities deliver total direct and diffuse radiation, direct sun duration, SVF and fisheye projections of sky obstructions | Geographical | 1993 | [47,48] |
| Kumar et al. | Direct clear-sky short-wave radiation for the DEM of a large area, latitude and time interval | Physical/ geographical | 1997 | [49] |
| RADIANCE | Light-backwards ray-tracing algorithm for direct radiation, diffuse and specular reflections from urban obstructions in a volumetric 3D model | Physical | 1994 | [50–52] |
| Cumulative sky approach | Global irradiance at the centroid of a scheme of patches 145 patches subtending a similar solid angle | Physical | 2004 | [54] |
| Daysim | Illuminance profile at each point in and around buildings using a daylight coefficient and RADIANCE-based backward ray-tracing | Physical | 2000 | [56,57] |
| ArcGIS Solar Analyst | ArcView GIS extension delivers a set of various radiation maps, fisheye equivalent photograph and a viewshed analysis | Geographical | 1999 | [58–62] |
| SRAD | Circumsolar radiation derived from within 5 degrees of the direct solar beam and an isotropic portion of the diffuse, monthly average cloudiness and sky view factor | Physical | 2000 | [63] |
| Solar Envelopes | A zoning device to achieve the largest volume that a building can occupy, regulates the development within limits of solar obstruction | Physical | 1976 | [64–66] |
| Albedo calculator and Albedo viewer | Simulation of albedos within 3D urban structures and web database | Physical | 2004 | [67] |
| ESRA clear-sky model | Beam irradiance at ground level from satellite images and data fitting techniques | Physical/ geographical | 2000 | [69,68] |
| *r.sun* | Irradiance raster maps, reflectance and shadow maps for horizontal or inclined surfaces, fitting to overcast and clear-sky conditions | Physical/ geographical | 1997 | [70–73] |
| RayMan | Detailed simulation for the short- and long-wave radiation flux densities from the three-dimensional surroundings | Physical/ geographical | 2010 | [74] |
| Preferable sky window | Sky section which has the greatest daylight potential in a horizontal plan located inside a building | Physical | 2009 | [75] |
| Tooke et al. | Fraction of incoming radiation that is transmitted through the semi-transparent vegetation canopy | Physical | 2012 | [76] |
| Solar3DBR | Google SketchUp plug-in for shading factor and the irradiation determination on surfaces of 3D models | Physical/ geographical | 2013 | [77] |
| SORAM | Direct and diffuse solar radiation incident on a sloping PV cell in an urban environment by ray-tracing | Physical/ geographical | 2014 | [78] |

#### 4.1.3. ATM

The first topographical solar model was the Atmospheric and Topographic Model (ATM) [38] which is a collection of UNIX-based tools and raster based programs within an image processing framework, not explicitly implemented within a GIS.

#### 4.1.4. Sky view factor

The sky view factor (SVF) was introduced to classify obstructions resulting either from 'self-shadowing' by the slope itself (known as shading) or from adjacent terrain (shadowing) [39]. A procedure to calculate the SVF is suggested in Tregenza [40], where the division of the sky hemisphere into small segments or sky zones is proposed. From this work, the International Commission on Illumination (CIE) recommended the use of a hemisphere evenly-distributed in 145 virtual light sources. Many other different sky subdivision strategies can be applied though (Fig. 3).

SVF is time independent, unless the environment at a certain point changes significantly, which may occur in cityscapes. Littlefair [42] reviews a range of tools to predict solar access in obstructed situations, including simple angular criteria, sunpath diagrams, solar gain indicators and solar envelopes, among others. It is important to highlight that SVF represents the solid angle of the visible celestial hemisphere normalized by the solid angle of the total celestial hemisphere, i.e. it considers only the geometrical aspect of the available sky radiation. Rakovec and Zakšek [43] explore different rationale for estimating diffuse radiation on a tilted surface, proposing a Diffuse Tilt Factor (DTF) which involves the integration of two different radiances over the two appropriate proportions of the solid angle. The DTF depends on the ratio of ground/sky brightness, which means that, for instance, if the surface tilt is high and the sky is brighter than the ground, more diffuse will reach the surface.

Vertical surfaces, however, require a special approach. Redweik et al. [44] determine the SVF along vertical facades by assuming that each facade point could see the whole sky hemisphere and that it is represented by a large number of light sources disperse all over the hemisphere [45]. The distribution of these light sources is approximately the third arrangement shown in Fig. 3, simulating in average the contribution of circumsolar radiation. The SVF of a particular point is obtained by knowing the number of times that a point has been lit and the total number of times it could have been lit. In a vertical facade point, the SVF is expected to be lower than 0.5, since generally only half of the sky hemisphere can be seen from a vertical facade.

#### 4.1.5. Solei-32

Introduced by Miklánek and Mészároš in 1993 and last updated in [46], Solei-32 calculates potential energy income to slopes with different orientations, daily solar irradiation, insolation duration and sunrise time from elevation data, cloudiness, albedo, turbidity

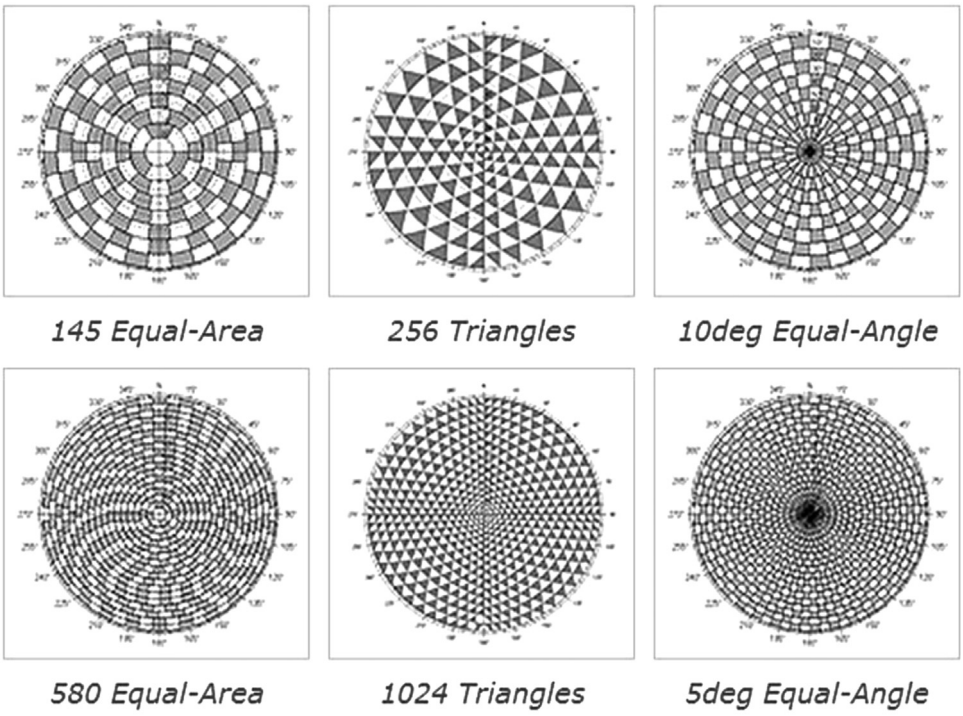


**Fig. 3.** Variety of sky division strategies to calculate SVF [41].

and optionally analyses shadow from surrounding topography and vegetation. First developed for DOS environment, the second version of the model was reprogrammed into the operating system Windows with FORTRAN programming language.

#### 4.1.6. SolarFlux

SolarFlux [47] was implemented in the Arc Info and Grid GIS platform as an ARC Macro Language (AML) program, providing access to a broad range of GIS capabilities. Through the input of a topographic surface, specified as a GRID of elevation values, latitude and atmospheric transmission, it delivers total direct and diffuse radiation, direct sun duration, SVF and fisheye projections of sky obstructions, with flexible temporal and spatial spans. The reflected radiation is not estimated. Moreover, the *hillshade* function can be used to simulate topographic shading and integration with the program CANOPY, simulating plant canopies. Through simulation of insolation for Big Creek Reserve, University of California, and other case studies with and without consideration of shadow patterns [48], the importance of topographic shading was confirmed.

#### 4.1.7. Kumar et al. model

Similar to SolarFlux [48], Kumar et al. developed a model [49] for direct clear-sky short-wave radiation in large areas, receiving a Digital Elevation Model (DEM), latitude and time interval. Also an AML language program, it has been implemented for commercially available GIS Arc Info and Genasys and was available online. Taking diffuse radiance as isotropic and ground surfaces as Lambertian, it achieves 3 × faster computation than SolarFlux, but it was found that errors in the DEM have great impact on calculated irradiance. It can be modified to include other parameters such as cloud type, percentage cover, thickness and altitude.

#### 4.1.8. RADIANCE

Applying the Perez diffuse radiation model [23] and considering both diffuse and specular reflections from urban obstructions, this software employs a sophisticated light-backwards ray-tracing algorithm based on the physical behaviour of light in a volumetric 3D model, including complicated curved geometries [50]. It is a powerful freeware, extensively validated and successfully used in applications related to solar potential estimates in building roofs and facades for electricity generation and daylighting analysis [51]. Another example of application of RADIANCE is the work of Robinson [52] who has used its unique abilities to model reflected radiation and an anisotropic sky to show that there is no linear relation between SVF and irradiance as it depends on the different materials, geometry of the canyons, etc.

This simulation software may be integrated as a plug-in in several design interfaces such as Autodesk Ecotect Analysis [8], DIVA4RHINO [53], among others.

#### 4.1.9. Cumulative sky approach

This is a method introduced by Robinson and Stone [54] to produce annual irradiation images from a single simulation. It is written in C language and is included in RADIANCE in the form of a module called *GenCumulativeSky*. It consists on the scheme based on Tregenza [40] in which each of 145 patches subtends a similar solid angle. The all-weather Perez model [55] is then used to predict the global irradiance at the centroid of these patches. It features an elegant balance between computational accuracy and efficiency.

#### 4.1.10. Daysim

Daysim is a validated RADIANCE-based daylighting analysis software. Employing a daylight coefficient method [56] based on ray-trace calculations and the Perez all-weather sky model [55] it generates an annual illuminance profile at each point in and around buildings. Ray-trace operations are achieved by taking a sky dome consisting of 145 diffuse sky segments, 3 ground segments and a second raytracing run with approximately 65 direct solar positions that are distributed along the annual solar path. By tracing backwards from the simulation sensor points,

each sky segment and solar position is then weighed relative to its contributions to each point in the scene [57]. Thus, any incremental time step is allowed while considering measured typical climate information, contextual shading and reflections based on a detailed three-dimensional geometric model.

A variety of Graphical User Interfaces (GUI) such as Autodesk Ecotect Analysis [8] can call Daysim from within.

#### 4.1.11. ArcGIS Solar Analyst

In the urge for expanded functionality, accuracy and calculation speed of radiation models, the Solar Analyst [58] was developed as an ArcView GIS extension, using C++ language (ESRI). The most relevant inputs for this model are location, elevation, orientation and atmospheric transmission. The radiation method consists in a geometrical approach that splits the sky into different sectors defined by their zenith and azimuth coordinates. Thus, considering either a uniform overcast sky (UOC) with the same incoming diffuse radiation from all sky directions, or a standard overcast (SOC) diffuse model, where diffuse radiation flux varies with zenith angle, this model computes a set of various radiation maps, fisheye equivalent photograph and a viewshed analysis similar to SolarFlux [48] and Kumar et al. model [49]. It is also a very flexible model in terms of temporal and spatial resolution. Many studies of solar resource and rooftop availability for photovoltaic setting up that used Solar Analyst and other tools from ArcGIS have been reported in literature [59–62].

#### 4.1.12. SRAD

This model, developed by Wilson and Gallant [63], analyses circumsolar radiation derived from within 5° of the direct solar beam and an isotropic portion of the diffuse component, as well as monthly average cloudiness and sky view factor. It takes into account slope, aspect, ground albedo, topographic shading and vegetation classification for each pixel of an image. SRAD computes short- and long-wave radiation components, the net irradiance, surface and air temperatures from inputs such as latitude, surface slope and aspect, monthly averaged atmospheric transmission or sunshine fraction, among others. It is freely available and runs on UNIX and, more recently, on Windows environment.

#### 4.1.13. Solar Envelopes

An insolation performance regulating tool, the Solar Envelope was introduced by Knowles about 30 years ago [64] as a zoning device to achieve solar access by regulating development within limits derived from the sun's relative motion, i.e. by calculating obstruction masks and shade projections the largest volume that a building can occupy is determined. Buildings within its boundaries will not shadow surrounding properties during critical energy-receiving periods of the day and year. The application of this concept to an urban area was guided using programs such as MascaraW [65], and Ratti and Morello [66] developed the 'sun isosurfaces', making solar envelopes more accessible for urban areas.

#### 4.1.14. Albedo calculator and Albedo viewer

These are two associated graphical user interface (GUI)-based applications that provide simulation of albedos within 3D urban structures, considering perfect isotropic return from multiple reflections (exchange of luminous energy between the whole of the elements of surface) and shading in the urban canopy [67]. *Albedo viewer* consists of a web application that offers access to a database of instantaneous calculations of albedo. Comparison with literature and observations reveal that calculated albedo is too high when sun is low, probably due to the isotropic assumption.

#### 4.1.15. ESRA clear-sky model

Consisting of a two-ways method for radiation and irradiation calculation at ground level, ESRA [68] uses the Heliosat approach [69] to derive that information from satellite images. Beam irradiance is constructed by knowing the Linke turbidity factor and the elevation of each pixel, and performing data fitting techniques rather than using shading masks, while the diffuse portion is the product of a diffuse transmission function at zenith and a diffuse angular function. No ground albedo was accounted for. The model was validated by ground stations data from different stations. It was coded in C language and was available online.

#### 4.1.16. r.sun

Conceptually motivated by the ESRA model, *r.sun* was developed as a clear-sky [70] GRASS GIS-based model, later improved [71] in order to overcome the limitations of some of the previously discussed models: Solei-32, SolarFlux, SolarAnalyst and SRAD, since these are not suitable for calculations over large areas. The *r.sun* model uses raster maps for terrain, latitude, turbidity, radiation and clear-sky index in order to produce irradiance and irradiation raster maps, reflectance and shadow maps for horizontal or inclined surfaces. It is fit to overcast and clear-sky conditions, defining diffuse transmission and altitude functions. Reflected ground radiation is considered isotropic and it is calculated through the definition of the fraction of ground viewed. This model works in instant time mode or daily mode, that can be used separately or in combination to provide estimates for any desired time step or interval. The model is optimized for European climate conditions.

Its most relevant and important contribution is the PVGIS online database [72]. An assessment of the PV potential of a small city in eastern Slovakia represents a significant breakthrough to the issue using GIS tri-dimensionally [73]. The representation of the digital elevation model and buildings constructed from footprints was attained using ArcView GIS. The *r.sun* model was then applied to estimate solar radiation and the electrical performance of PV components simulated using PVGIS. At this stage, only rooftops' solar potential was considered.

#### 4.1.17. RayMan

The RayMan model is a Windows-based software written in Delphi [74]. Built for human thermal comfort analysis, it is a detailed simulation for the short- and long-wave radiation flux densities from the three-dimensional surroundings in simple and complex environments. Sunshine duration and shadow are also included, accounting for atmospheric attenuation effects in the direct radiation and both isotropy and anisotropy of the diffuse radiation are taken into account. Basic meteorological data such as air temperature, air humidity and wind speed are needed for input, as well as albedo and emissivity of the different solid surfaces.

#### 4.1.18. Preferable sky window

This is a technique used to evaluate daylighting availability in different urban scenarios; it identifies the sky section which has the greatest daylight potential in a horizontal plan located inside a building. The Preferable sky window concept considers the sky hemisphere patches, the light incidence angle and the indoor sky visibility to calculate the equidistant projection as a SVF. It is explored using an Apolux code in Pereira et al. [75].

#### 4.1.19. Tooke et al.

Tooke et al. [76] proposed a method based on gap probability analysis to determine the fraction of incoming radiation that is transmitted through the urban vegetation canopy, contrarily to

simple solid shadow casters. It confirms the importance of accounting for the semi-transparent nature of vegetated features when modelling irradiance on urban facets such as ground, roof and walls. Through multiple LiDAR signal returns, that represent several levels of penetration through the canopy, a vegetation extinction coefficient and a probability density function for each tree cell can be defined. An isotropic sky was considered but the reflected component was excluded. The method is best suited to the vegetation condition at the time of the LiDAR acquisition, since no temporal, spectral and structural dynamics of the local vegetation is taken into account.

#### 4.1.20. Solar3DBR

The study of the shadows projected by nearby buildings and other elements around a PV surface was simulated in Melo et al. [77] and compared to a real experimental set up. For this purpose, a methodology to estimate the shading factor and the irradiation on surfaces of 3D models is proposed, taking into account simplifications introduced in the Perez model [20]. The creation of a shading matrix containing direct shading factors and shading impacts on direct beam, isotropic, circumsolar and horizon brightening diffuse solar radiation components allows good precision and simplicity, with faster calculation times, which is important for making this approach suitable for web-based applications.

The Solar3DBR was developed as plug-in deployed to Google SketchUp, permitting the increase in the representation details, as well as reduced modelling process time.

#### 4.1.21. SORAM

Erdélyi et al. [78] evaluate the direct and diffuse solar radiation incident on a sloping PV cell in an urban environment. This is addressed by combining a refined version of the anisotropic model [23], making it able to ray trace the angle of incidence for each diffuse ray. Knowing that each solar ray contributes differently, according to its origin in the sky dome, diffuse radiation from a patch in the sky is transformed into a specific ray, likewise the computation of a SVF. The proposed algorithm computes the dynamic 3D shading from urban obstacles, such as buildings or trees. However, no reflected radiation is considered.

A validation attempt is conducted using empirical measurements from two pyranometers installed in a sample area; both at a 12.7° tilt, one facing southeast and the other southwest. The edges of the sampled buildings were introduced based on Google Maps and the obstacles, such as surrounding buildings and trees, were approximated by voxels. Results show that SORAM overall performs better than the enhanced Perez model.

#### 4.1.22. Model comparison

Ruiz-Arias et al. [79] compared four DEM based models for a Mediterranean environment characterized by a complex topography: Solar Analyst, *r.sun*, SRAD and Solei-32. Both clear sky and overcast conditions were accounted for, as well as two DEM spatial resolutions, 20 m and 100 m. Results from the comparison with measured data from several stations show that *r.sun* and Solei-32 perform best, with root mean square errors (RMSE) around 15% and mean bias error (MBE) under 10%. Reliability increases with higher spatial resolution for clear-sky situations, but decreases for overcast. This is consistent with the fact that for overcast conditions almost all the solar radiation is diffuse, which is less sensitive to the surrounding topography than the direct radiation, thus being more difficult to estimate.

One main conclusion that could be drawn is that experimental data should be used in order to accommodate the estimates to the actual values. The approach followed by Solar Analyst and SRAD consists on the use of the observed data to parameterize the state of the atmosphere before the estimate is provided, whereas *r.sun* and Solei-32 use the observed data to correct the estimate. The latter revealed more consistent estimates.

It is also interesting to highlight that in the cited study, as an area of about 50 $km^2$ was surveyed, the required computational resource was very dissimilar among models, ranging from 100 to 1500 s per run, considering the 20 m resolution DEM.

### 4.2. Solar potential urban-oriented models

Large areas and tri-dimensional phenomena in urban scenarios require more complex models to associate a 3D urban construction to calculations based on physically-based formulations of the solar radiation, as addressed before. However, the representation of numerical results proves to be all but trivial in complex built environments. One of the most challenging issues regarding urban models is the representation of vertical elements and the storage of information on each cell. Most design methods extrude buildings in height from footprints, resulting on a vertical surface represented by a single valued function. This practice originates a 2.5D model, where for each planimetric ($xy$) position there is only one height ($z$) [80]. Likewise, the 3D point cloud obtained from Laser Scanning can be aggregated to 2.5D raster cells leading to an irreversible loss of the third dimension as well. In analysis that do not require this third dimension, this approach is adequate as it is less time consuming, but when it comes to solar potential assessment of facades that is evidently not the case, because it fails in the determination of solar radiation for points on facades, embodying a discontinuity in a 2.5D DSM [81]. The third dimension can be included if proper facade modelling is done, which is inconceivably time-consuming if applied at the whole city scale. This technique is mainly used when modelling individual buildings and detailed architectonic elements.

A different approach was employed by Jochem et al. [82] that, by means of a Mobile Laser Scanning (MLS) survey, estimated the solar potential of buildings' facades. Using *r.sun* [71] it sums diffuse and direct radiation to determine global radiation. Shadows were obtained by the definition of a searching radius for nearby objects to project the 3D horizon of each point of a facade segment within the 3D GIS-ready data point cloud. However, a proper treatment of MLS data is required, for only the surfaces that are facing the street were surveyed and point collection is incomplete due to trees, window curtains and other objects non-transparent to the laser wavelength.

Any 3D model can be represented in different Levels of Detail (LoD), ranging from 0 to 4 [83], according to the purpose of the analysis. The lowest LoD contains only the representation of the terrain, while LoD 1 features buildings represented by basic parallelepipeds, LoD 2 includes the slope of rooftops, LoD 3 has facades elements modelled and the highest LoD features the interior of the buildings.

Several of the more sophisticated models in the last decade, developed specially focused on estimate solar potential in urban environments, will now be explored.

#### 4.2.1. All-in-one models

Tools that couple modules for solar radiation treatment with design interfaces or 3D object representation in a single software are here classified as all-in-one models. Although featuring user-friendly work environments, these models allow reliable quality assessments at small and medium scale.

*4.2.1.1. TOWNSCOPE.* TOWNSCOPE II was a follow-up of the earlier model CAM.UR (Computer Aided Management System for Urban Renewal) developed in the 80 s by the LEMA research group at the University of Liege, Belgium [84]. This upgrade, adapted to Windows

instead of UNIX workstations, consists on software developed to support solar access decision-making in a sustainable urban design perspective and helped achieving several objectives of the POLIS project 1996–1998. It was applied to a number of case studies, including the LISBOA'98 international exposition, in Portugal, and a central urban located open space, the place Saint-Lambert, in Belgium. The software consists of 3D urban information system coupled with solar evaluation tools, morphological and wind risk analysis tools.

In TOWNSCOPE, 3D volumes are represented as 3D point, polyline, border, face and volume, applying a triangulation to define ground and other irregular surfaces. Volumes are described through their constituting faces, which means that holes may not be described. The 3D objects can be acquired either via solid modellers, such as AutoCAD, or direct data acquisition tools. Once the model is completed, the data-processing tools calculate the direct, diffuse and reflected solar radiation on any point or face defined by the user. On the basis of stereographical projections, the masks of shade and thus the sunshine duration can also be evaluated for any specified point. Moreover, evaluation of human thermal comfort in an urban open space as well as sky opening, view lengths and visibility analyses provide perceptive qualities of urban open spaces.

The solar assessment analysis consists in methods for obtaining hourly radiation in a clear site from latitude, altitude, humidity and turbidity information, or more precise meteorological data, if available. Direct component calculations are based on analytical geometry equations made on the sphere, considering partial solar masks, through transmissivity and diffusion factor applied to the volumes, and possible density of foliage. Diffuse radiation is assumed to be isotropic, to which SVF and a sky component factor based on the CIE standard overcast conditions are calculated. Reflected radiation is computed from surrounding faces considering view factors, isotropy and one inter-reflection. Specularity is not included. A newer version of the software is commercially available [6].

*4.2.1.2. SOLENE.* To overcome some limitations of the existing tools, such as restrictive conditions about the input geometry, limited sky conditions, and a separate approach for indoor and outdoor spaces, SOLENE, a set of numerical models for the simulation of natural light in the urban morphologies was created by CERMA, in the Research Laboratory of Nantes School of Architecture, France [85]. It works on Windows OS with OpenGL as visualization libraries and a user interface written in C++ language.

The sun is modelled by a geometric approach and energy is given by a statistical radiance model, to which the solar constant, altitude, eccentricity, air mass, turbidity, among others, must be described. The sky vault can be seen as a source of diffuse radiation, anisotropically distributed. The all-weather Perez model [55] is employed, with further implementation of conventional CIE overcast and clear skies, and a geodesic triangulation of the hemisphere in patches is used for computation and visualization.

SOLENE is suited to compute radiation in a small set of buildings and streets, or possibly in a small-sized district, using as input the 3D meshed geometry of the scene, the nature of the used materials and their physical parameters. This allows thorough exploration of the physical behaviour of light. Emphasis is given to the processing of transparencies and, using a multi-reflection method, the importance of the middle area of the facades in the multi-reflexion process in an urban street is highlighted. However, other types of material dependent reflections, from ideal diffuse to ideal specular, and incorporation of semi-transparent screens of vegetation, with a species dependent transmissivity and seasonality, will be subject to further model improvements.

SOLENE has been used to analyse different case studies, to evaluate outdoor conditions and external comfort beyond lighting, such as in the historical heart of the city of Toulouse [86] and in an urban fabric representative of the 19th century in Marseille [87]. Both studies pointed out that this thermo-radiative model is an efficient and scale-flexible way to analyse the various aspects of the urban microclimate in detail.

### 4.2.2. CAD plugin-based models

Contrarily to the models in the previous subsection, which receive the 3D objects but also have their own design modules, recently some CAD plugin-based 3D modelling software have been developed. They receive plug-ins from other software able to conduct radiation analysis, are very versatile in the non-urban/urban context analysis, performing with great detail and user-friendly commands.

*4.2.2.1. Skelion.* Skelion [7] was created in 2011 by Juan Pons and Sam Jankins as a plug-in for Google SketchUp. It performs a simulation of the electrical output power of a number of PV components added to a certain design. Solar obstructions can be projected over the roof with a distance/height or a solstice shadow criterion to determine the area that accomplish the purpose. Georeferenced building and terrain can be imported from Google Earth. Solar radiation and the subsequent electrical PV production estimates are acquired from the PVGIS database or from PVWatts, depending on the location of the structures. When using PVWatts, Skelion further calculates the shading derate, the percentage of solar energy available for each panel taking into account near shadows. If modelled, trees are considered as solid shadow casters. The output is delivered as reports containing the components and energy yield, arranged either by face, or by groups with the same component, slope and aspect, or by arrays.

In spite of being a functional tool to quickly build good looking designs with PV installations, here the third dimension is somehow lost, since solar radiation databases cannot provide values in height for different elements on a facade, hence not making it possible to conduct shadow analysis on these features.

*4.2.2.2. Autodesk ecotect analysis.* This software is the combination of numerous detailed analysis functions with a highly visual and interactive display that presents analytical results directly within the context of the 3D model. It was developed by Square One Research, acquired by Autodesk in 2008 and is commercially available. Ecotect follows a split-flux model of daylighting, featuring several applications, such as solar radiation on windows and surfaces showing differential incident radiation calculated over any period using longitude, latitude and climate file as inputs. It also displays the position of the sun and its path relative to the input model at any date, time and location and it shows how sunlight enters through windows and moves around within a space, calculating daylight factors and illuminance levels at any point, among many others [8]. The final results can then be assigned to the objects in the model as attributes. However, the method for calculation of solar radiation on the surfaces has not been disclosed. A comparison with measurements in Vangimalla et al. [88] show that Ecotect cannot be used for accurate simulations of thermal loads and illuminance levels.

### 4.2.3. GIS-based models

The most sophisticated models to predict the physical potential of the solar resource at the large scale of the urban fabric are addressed in this section. Models that rely on GIS to represent the outputs of radiation algorithms applied to surface data are described and briefly summarized in Table 2.

*4.2.3.1. Carneiro et al.* This work started by the development of a 2.5D urban surface model (i.e. a 2.5DSUM) from LiDAR data, 2D vectorial digital maps of buildings footprints and altimetric information about buildings' heights in the city of Geneva,

**Table 2**
Overview of the more sophisticated urban-oriented 3D models.

| Model | Surfaces | Radiation input | Topographic input | Radiation model | Resolution | Software | Highlights |
|---|---|---|---|---|---|---|---|
| Carneiro et al. [9] | Flat and tilted rooftops, facades are sliced every 3m | MeteoNorm database: average monthly irradiation | Airborne LiDAR, buildings footprints, buildings' heights | Hay model, SVF | 1 h<br>0.25 $m^2$<br><br>2.5D/3D pixel-based | Several GIS<br>Raster image processing<br>MatLab | • Straightforward approach<br>• Low representation detail<br>• Requires automation |
| *v.sun* [10] | Flat rooftops, vertical facades | Satellite images: raster maps | Photogrametry | *r.sun* | 1 h<br>2.5 m voxel<br>3D vector–voxel polygons | GRASS GIS | • Open-source code<br>• High model detail»high computation time<br>• No land surface or trees between the buildings |
| Jakubiec and Reinhart [11] | Detailed rooftops, tilted surfaces | Boston Logan TMY3 | Airborne LiDAR, oblique images | Perez model, cumulative sky method | 1 h<br>1.5 $m^2$<br>3D triangulation | Radiance/<br>Daysim | • Diffuse reflectance for different materials is considered<br>• Limited geometric accuracy<br>• Trees are solid shadow casters |
| *SOL* [12] | Detailed rooftops, vertical facades, tilted surfaces | SolTerm database (altern.): hourly Direct and Global radiation | Airborne LiDAR | Kumar model (altern.), SVF with non-uniform grid | 1 h<br>1 $m^2$<br>3D pixel-based and multi-patch | MatLab ArcGIS | • Outputs detailed shadow and irradiance maps for all surfaces<br>• Limited geometric accuracy<br>• Trees are solid shadow casters |

Switzerland [9]. All surfaces with slopes greater than 60° were considered as being vertical surfaces. The solar radiation in roofs and building facades is estimated using Hay's anisotropic model [19]. Running a Matlab routine, hourly direct and diffuse radiation incident in any surface slope and aspect was calculated for clear-sky conditions. Reflection from proximities was also included, as well as a shadow and SVF algorithm to account for the effects of the surrounding built environment. The latter was calculated based on Ratti's algorithm [45], already explored in Section 4.1.

As seen earlier, facades incorporate points that have the same *XY* position but different *Z* heights. This limitation was somehow overcome here using a 3D urban model with its facades sliced at regular height levels, every 3 m, representing approximately the height at each level. It is important to highlight that to each of those slices only one attribute is assigned.

The electrical energy produced was obtained by multiplying the global irradiation incident on a given roof section by the installed power of a given PV panel and a performance ratio. Solar thermal evaluation was also performed.

Data from Meteornorm consisting in average hourly irradiation for each month of a typical year were used for each pixel of a high resolution 2.5DUSM. If hourly values of radiation over one year had been used instead, the computation time would be in the order of several days. The results of the whole algorithm were plotted graphically, with facade bi-dimensional visualization and roof in tri-dimensional, in LoD 0, 1 or 2. In Fig. 4, the LoD2 representation of yearly irradiation can be observed. Data query can be done at the facade or total building level.

*4.2.3.2. v.sun.* The *v.sun* module [10] for vector-based data, implemented in GRASS GIS, is based on the existing solar radiation methodology used in the topographic *r.sun* model [71] with a new calculation procedure based on the combined vector–voxel [89] approach to process 3-D vector data representing complex urban environments.

The shadowing effects of surrounding objects are taken into account using a unique shadowing algorithm considering the effects of neighbouring buildings. As some facades or roofs can be partially shadowed, the original 3-D polygons representing these surfaces must be segmented to smaller elements to attain spatial variation of a certain attribute such as solar radiation. A perpendicular projection of segmentation polygons to the solar ray vector is calculated either using a voxel bit mask or a projection technique. The already cited Tooke et al. [76] approach to represent attenuation due to vegetation canopy can also be easily implemented in the *v.sun* model, using voxels representing an attenuation factor.

The step of solar radiation computation delivers the three components: beam, diffused and reflected radiation, for clear- or real-sky conditions, and the results are saved to an attribute table of polygon elements.

Smaller voxel size provides more spatial details and higher estimation accuracy but calculation time is inversely affected. It is a free, open-source program with available source code for further improvement.

The applicability of the model was demonstrated for the urban area of Presov, Slovakia. The 3D city model of this sample area was derived from the photogrammetric method and the LoD1 city model was chosen, as it is considered to be sufficiently adequate to the objective but faster to process. Results highlight strong spatial and temporal variation of solar radiation flows over the surfaces. An example of the clear-sky irradiation calculated for July in Presov is shown in Fig. 5.

*4.2.3.3. Jakubiec and Reinhart.* This model first approaches the creation of a comprehensive 3D model using the validated


**Fig. 4.** 2.5DSUM with representation of the annual solar irradiation by roof sections for a region in Geneva [9].

Radiance/Daysim backward-raytracing daylight simulation engine. In Jakubiec and Reinhart [11] a 3D representation of the city of Cambridge, USA, is derived from a LiDAR survey uniformly resampled over a plan grid. Then, using GIS datasets from the city, buildings and ground were separated into two categories of points to be triangulated using a Delaunay algorithm. The result was converted into the proper format and coordinate system to input in Radiance.

Building walls were taken as Lambertian diffusers with a 35% reflectance while the surrounding landscape has a diffuse reflectance of 20%. The reflectances and absorptivities of rooftops were calibrated according to the rooftop material. Roof surfaces sloping greater than 60° were considered as vertical surfaces or walls but the model could model facade integrated photovoltaics by generating simulation sensors on such wall surfaces.

The detailed Perez sky model [55] and the cumulative sky method are employed in irradiation simulations performed at an hourly timestep with Daysim, in a 1.5 $m^2$ grid. Hourly averaged global horizontal irradiation and air temperature from a nearby weather station were used. Direct contribution is sampled for each ray reflection, considering up to two ambient reflections from direct solar irradiation and one reflection from diffuse sky irradiation from the environment. In Fig. 6, an illustrative irradiation map for the studied area is presented.

The efficiency of simulated PV devices is based on the calculation of sol–air temperature, i.e. the air temperature near urban rooftops that accounts for the effects of convection and absorptivity on the surfaces plus the ambient temperature. The panel temperatures can be calculated relying upon knowledge of the Nominal Operating Cell Temperature (NOCT) and a de-rating factor based on temperature correction. The model resolves this efficiency loss on an hourly basis.

The model's accuracy was demonstrated through the comparison of real rooftop PV systems installed in a nearby student centre and a residential building and simulations from Daysim, SolarAnalyst, *r.sun*, PVWatts and a solar constant methodology. Results show annual errors ranging from 3.6% to 5.3% for the present model, which is smaller than inter-annual variations in predictions for PV electrical generation.

*4.2.3.4. SOL.* SOL is an algorithm created in Matlab environment for the assessment of solar potential in the urban environment at any point of an urban landscape regardless of its location on a roof, ground or facade [12]. The methodology starts from a georeferenced LiDAR data cloud, re-sampled for a $1 \times 1\ m^2$ raster. Pixels with a slope greater than 72° were set to 90°, as they might correspond to vertical walls in an urban environment.

The local typical meteorological year (TMY) data set associated to the SOLTERM database was used. This includes hourly mean values for horizontal direct and diffuse irradiation calculated over 30 years from climatic observations. To obtain the irradiance on tilted surfaces a geometrical approach based on the position of the sun is employed, although, empirical solar radiation models such as Kumar et al. [49] could be used instead.

At every instant, a shadow algorithm takes each point of the Digital Surface Model (DSM), including trees, as a shadow caster along the line opposite to the direction of the sun [81]. If this line is interrupted, i.e. when a DSM cell along that line features a *Z* value lower than the shadow line at that position, the pixel is in shadow and receives the attribute 0, in order to create a binary map. The SVF method of Ratti and Richens [45] was applied, including a non-uniform disposition of light sources representative of the circumsolar diffuse irradiation. Points in facades correspond to hyperpoints, which are composed by a certain number of points with the same *XY* but different *Z* coordinates. Since at any time, a hyperpoint in the facade can be totally in shadow, partially in shadow or totally sunlit, the model has a special treatment for their SVF.

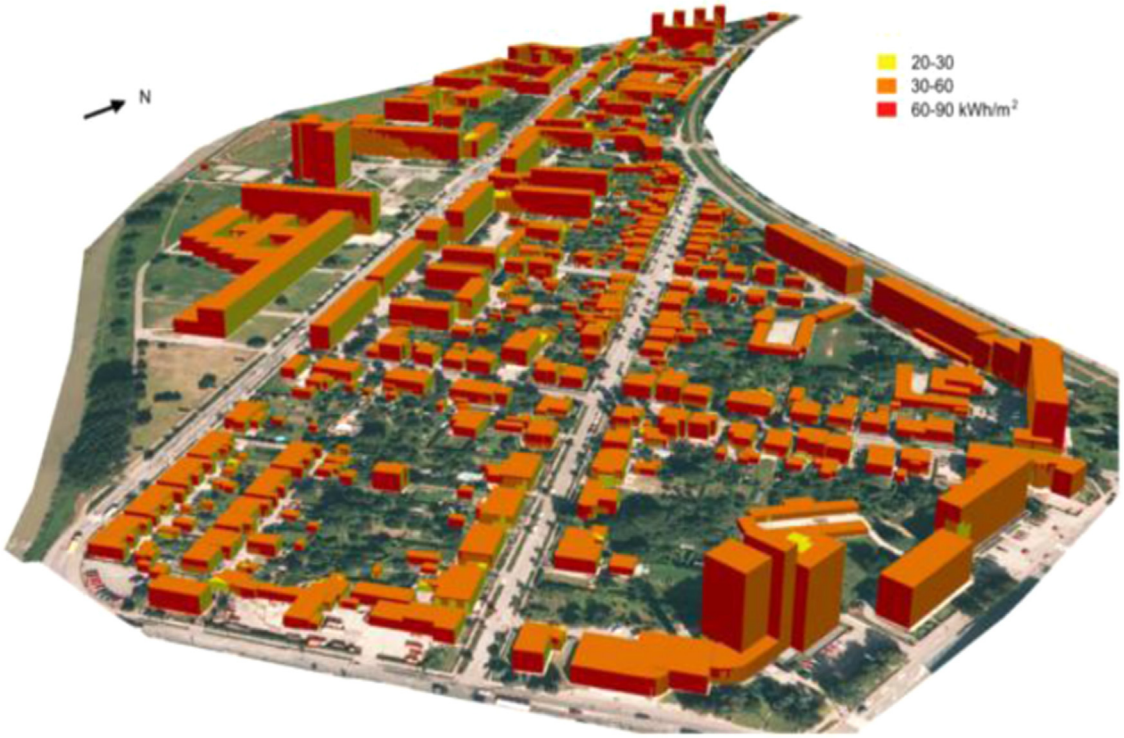


**Fig. 5.** Global clear-sky solar irradiation estimated for July in Presov [10].

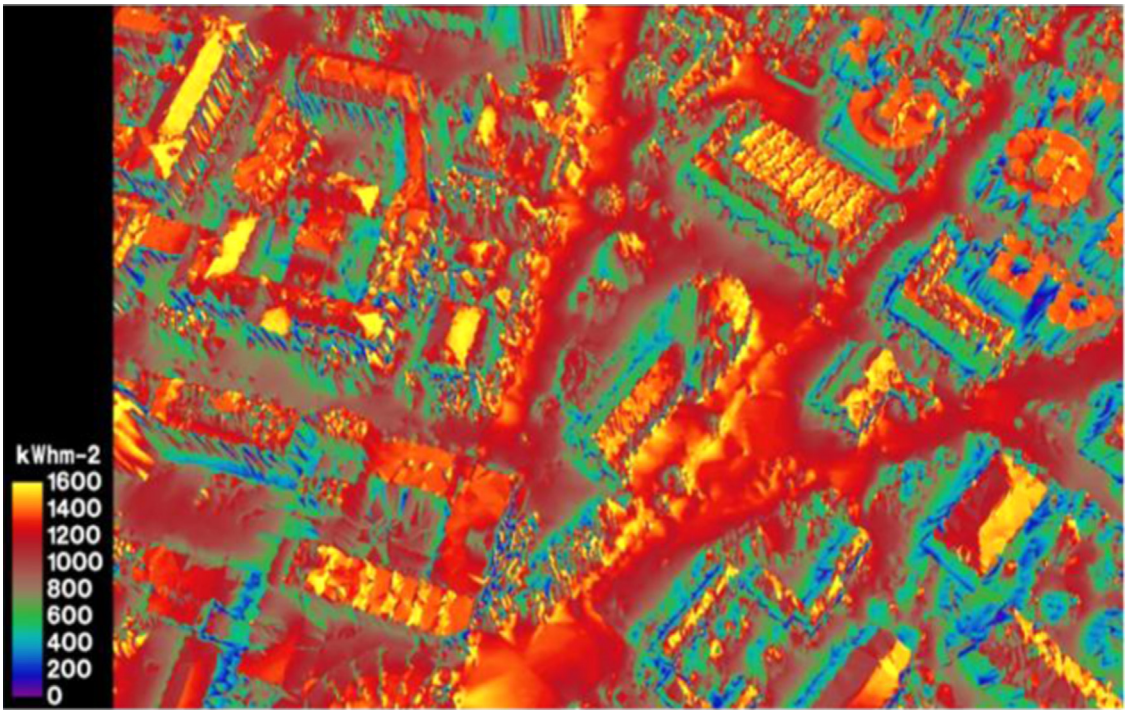


**Fig. 6.** Annual irradiation map for the city of Cambridge when considering detailed rooftop representation [11].

A case study for the Faculty of Science of the University of Lisbon (FCUL) campus showed that the south oriented facades receive a larger amount of solar irradiation than the roofs in the winter, the reverse being observed in the summer. Facades show smaller seasonal variations than roofs. As an illustration of the model output, Fig. 7 shows the distribution of yearly global irradiation.

### 4.3. Web-based solar maps

After having explored the solar potential assumptions and calculation methods discussed in the literature, it is important to assess how can those models help in the resolution of field-related issues. A solar map or cadastre typically consists on a web-based interface that visually represents a specific location and provides

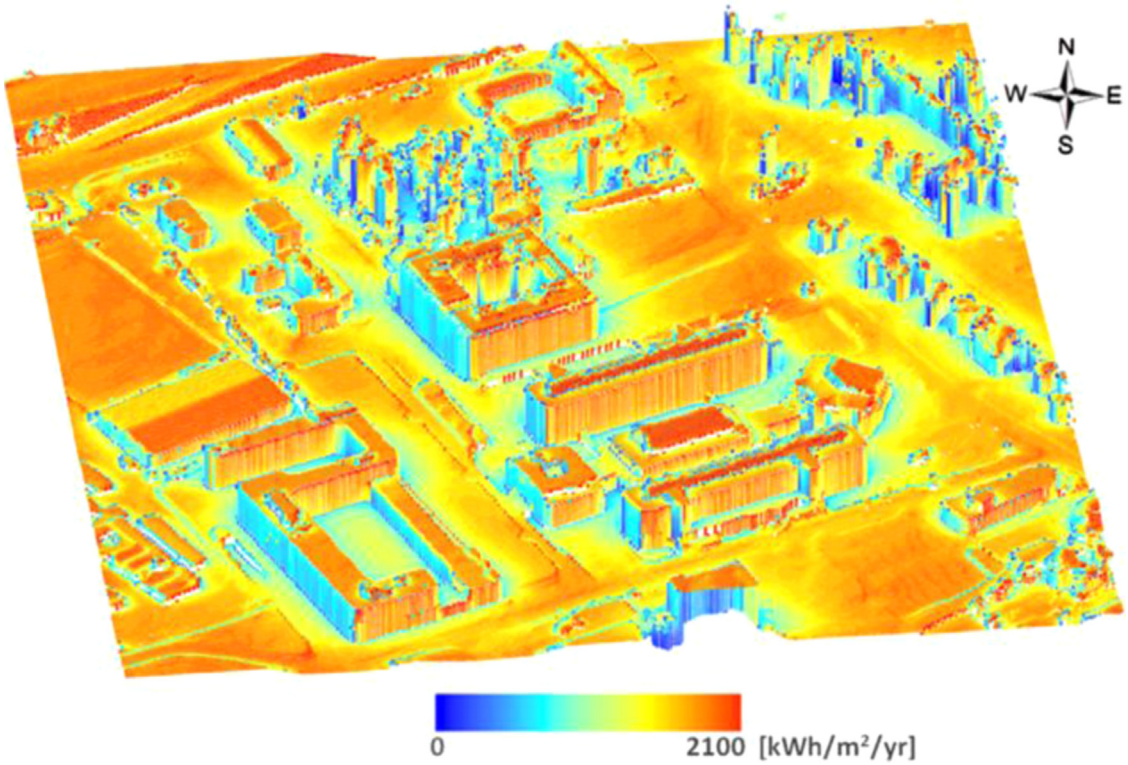


**Fig. 7.** Yearly global irradiation in the Faculty of Science of the University of Lisbon campus [44].

information, such as solar irradiation, estimated PV system size, projected electricity production, to be queried and gathered. Solar maps should be user-friendly, instructing the user about the benefits of solar PV and its associated costs, and corresponding savings. Surveys and reviews of solar maps existing in the US can be found in [11,90]. The most relevant and state of the art examples are briefly described below. Table 3 presents a more complete list of solar maps publicly available.

#### 4.3.1. PVGIS

The well-known PVGIS database presented in Huld et al. [91] allows the visualization of solar radiation data for Europe, Africa and South-West Asia, with a resolution of 1 km. The tool calculates solar radiation using the *r.sun* model, using ground-based measurements for Europe (1981–1990 data) and Africa (1985–2005 data) and defining clear-sky coefficients. It includes terrain shadowing losses. The interface allows the user to input nominal peak power, estimated losses, orientation and inclination, mounting type, technology used, among other features. The output include optimum panel inclination for a given location, monthly and yearly global irradiation maps, daily irradiance profiles, climatic parameters and potential PV production, considering ambient temperature.

This solar map also lets the user choose between the older or a more recent solar database, based on CM-SAF satellite data, i.e. solar irradiance data derived from instruments on board the Meteosat satellites. Although mountain areas may still incorporate a significant level of uncertainty, the newer database has a minimum bias deviation (MBD) of +2%, whereas the older has +5% [92].

#### 4.3.2. PVWATTS and In My Backyard

The solar mapping tool PVWatts [93] was firstly available only for the USA. Combining data from the TMY2 with a topographic model with a spatial resolution of 40 km$^2$, the calculator tool PVFORM and the Perez anisotropic diffuse model are used to estimate annual PV production and its value in dollars. Newer versions, extending the model for any location in the world, allow the user to search for an address, postal code or geographical coordinates, and set input information such as local electricity costs, tilt and surface azimuth, tracking mode, DC rating and a de-rating factor. This tool is currently undergoing further development.

Another tool to access PV potential with a map-based interface that allows the user to specify an address or manually select a rooftop is *In My Backyard* [94]. An hourly satellite-derived data set with a spatial resolution of 10 km is used to calculate the solar resource. Using a modified version of PVWatts and DSIRE database of renewable incentives and taxes, it estimates the electricity produced by a PV system over a year, including hourly AC output, its value, payback and contribution to the load profile. It will be discontinued and incorporated in a yet to be released new version of PVWatts.

#### 4.3.3. Mapdwell Solar Systems maps

One example of state of the art solar map is the Cambridge Solar Map, which was created under the scope of Jakubiec and Reinhart [11] model. The same methodology also originated the Mapdwell Solar System's map in Washington, DC.

Both maps include building rooftops and structures, existing infrastructure, and tree foliage. The user can search for an address or manually select the roof of interest and/or change its size. Areas with lower solar potential are excluded. For a queried rooftop, results include financial, technical and environmental information such as cost to owner [$], monthly revenue [$], system size [kW], payback period [yr], and carbon offset (trees per year). A coloured code also help visualizing roofs defined as "poor", "average", "good" and "optimal" or not available at all.

A ±3–5% margin of error is stated, which is attributed to inaccuracies due to partial sample obsolescence, excess of vegetation or non-modelled obstructions, incomplete or corrupted

**Table 3**
Solar mapping tools worldwide developed.

| Solar map | URL | Method |
|---|---|---|
| PVWatts | http://pvwatts.nrel.gov/ | PVForm |
| Anaheim City | http://anaheim.solarmap.org/ | Solar Analyst |
| Berkeley | http://www.cityofberkeley.info/solarmap/ | Flat Roof Constant |
| Boston City | http://gis.cityofboston.gov/solarboston/# | Solar Analyst |
| Cambridge City | http://en.mapdwell.com/solarsystem/cambridge | Radiance/Daysim |
| Denver Regional | http://solarmap.drcog.org/ | Unknown |
| Green Riverside | http://www.greenriverside.com/Green-Map-9 | Unknown |
| Los Angeles Country | http://solarmap.lacounty.gov/ | Esri Solar Analyst |
| Madison City | http://solarmap.cityofmadison.com/madisun/ | Unknown |
| Milwaukee | http://city.milwaukee.gov/milwaukeeshines/Map.htm | Unknown |
| New Orleans | http://neworleanssolarmap.org/ | Unknown |
| New York City | http://www.nycsolarmap.com/ | Solar Analyst |
| Orlando | http://gis.ouc.com/solarmap/index.html | Unknown |
| Portland | http://oregon.cleanenergymap.com/ | Unknown |
| Sacramento | http://smud.solarmap.org/ | Unknown |
| Salt Lake City | http://www.slcgovsolar.com/ | Solar Analyst |
| San Diego | http://sd.solarmap.org/ | Unknown |
| San Francisco | http://sfenergymap.org/ | Flat Roof Constant |
| Santa Clara Country | http://www.svenergymap.org/ | Unknown |
| Sonoma Country | http://www.sonomacountyenergy.org/ | Unknown |
| Tallahassee | http://www.talgov.com/you/you-learn-utilities-electric-solar-map.aspx | Unknown |
| Washington DC | http://en.mapdwell.com/solarsystem/dc | Radiance/Daysim |
| PVGIS | http://photovoltaic-software.com/pvgis.php | *r.sun* |
| Lisbon | http://lisboaenova.org/cartasolarlisboa | Unknown |
| Berlin | http://www.businesslocationcenter.de/wab/maps/solaratlas/ | SUN-AREA |
| Bristol | http://maps.bristol.gov.uk/pinpoint/?service=localinfo | SUN-AREA |
| Osnabrück | http://geo.osnabrueck.de/solar/ | SUN-AREA |
| Braunschweig | http://geoportal.braunschweig.de/ASWeb33/ASC_Frame/portal.jsp | SUN-AREA |
| Gelsenkirchen | http://geo.gkd-el.de/website/solar/viewer.htm | SUN-AREA |
| Scharnhauser Park | http://www.polycity.net/GIS/ | SUN-AREA |
| Australia | http://pv-map.apvi.org.au/historical | CUNY |

databases, incomplete or corrupted GIS layers, or undetectable partial obstructions based on survey resolution.

## 5. Discussion

In spite of great progress associated to emerging interest and increased computer power, the survey of the different models showed that there are still many limitations that require further development. Firstly, it has to be underlined that the level of accuracy must agree among the several input data that are required to run a simulation. For example, in the case of PVGIS the major source of uncertainty comes from the quality and the spatial detail of the input data used in the models, in particular parameters such as atmospheric turbidity, ozone, water vapour, aerosol optical depth, that may not match adequately the DEM's [95]. Also the use of data from different periods and differences in accuracy between interpolation from ground station measurements or satellite derived must be mentioned. Of course, higher temporal and spatial resolution would help to improve the database.

At the input level, LiDAR data also presents limitations. Redweik et al. [96] highlight errors revealed by this type of data, mainly in some of the facades which are very close to each other, attributing this circumstance to multi-path effects in the LiDAR survey.

Some radiation models, in spite of the awareness of an incorrect isotropic representation of the diffuse and reflected radiation, still adopt this simpler methodology as a compromise between acceptable results with reasonable computation time [47,49,63,67,71,76]. RADIANCE, Daysim and SOLENE are certainly some of the best software capable of performing detailed simulation of light anisotropy and specularity, as well as inter- and multi-reflections.

Further challenges arise from the representation of the surfaces themselves. In the case of more basic models, the fact that slope or aspect may not be considered is immediately a critical limitation. Moreover, many models consider flat surfaces, which means that items such as chimneys, air-conditioning units or other structures are left out. In more general terms, the modelling of windows in facades not only lack proper representation of its elements but also appropriate assessment, since this requires the development of complementary analysis based on photogrammetric methods, for urban scale analysis, or local technical assessment for a particular facade.

Vegetation in the urban context is often simplistically considered as solid shadow casters, frequently even excluded, but procedures for their selection from a LiDAR point cloud data are emerging together with proper algorithms for their treatment. Much effort is still needed in this area of research, in particular as far as the representation of trees and light passing through their canopies in 3D models is concerned.

Conversion of solar radiation to electrical output from PV panels can be performed within the model itself or implemented in a second step, using other PV simulation software. It is essential to provide and account for ambient temperature and/or module temperature when estimating PV production. PVGIS considers the first and Jakubiec and Reinhart [11] estimate the second based on the previous calculation of sol–air temperature. As far as solar thermal potential is concerned, the analysis must entail estimates of local demand, e.g. from population distribution, as the conversion efficiency depends on demand [97].

A major challenge is the development of validation procedures for the models as a whole. Despite the extensive tradition of empirical radiation model validation, this new approach to georeferenced 3D urban solar potential models requires more demanding validation procedures. To validate a model, a significant amount of case studies is required, since the outcomes are site and technology dependent due to the amount of complex phenomena involved. On the other hand, there are not many measurement systems (e.g. pyranometers) installed in complex urban scenarios or BIPV spread into the cityscape, to provide reference data. Thus, it is expected that, as further and more

sophisticated solar maps and further and more diverse installation case studies are published, an interactive dialogue between these two research areas will lead to model validation and improvement.

Emerging trends provided by more sophisticated modelling tools are mainly concerned with applications in larger urban areas. Attentions are also turning to holistic assessments on which application is the most cost-efficient for a certain design or agglomerate [98]. Beyond solar PV, there can be more adequate conditions for other energy analysis goals, such as solar thermal, daylighting, ventilation, etc., that can be accounted for.

Regarding solar mapping limitations, the importance of updating LIDAR scan data is critical. There is always the risk of providing outdated data, broken links and inaccurate depictions of the prevalence of solar in communities. On the other hand, installation requirements and regulatory limitations include a number of criteria that often cannot be evaluated based on available data alone, and therefore the usable area on any rooftop is likely to slightly differ from the estimate.

Owners of solar PV installations have a role to play as well, for it is their contribution that allows the monitoring of the PV input to the electric system. Nevertheless, these maps tend to employ very simplistic solar assessment methodologies, frequently simple interpolation of ground station measurements, causing the results to be inaccurate. Examples of more refined methods allied to user-friendly maps are the Washington, DC, San Francisco and Los Angeles solar maps.

Finally, emphasis must be given to the fact that the costs associated with map development against the benefits must be wisely weighted.

After great advancement in 2D solar mapping, GIS tools are now progressively adapting to detailed 3D representation and spatial analysis, which is not trivial [99] and is yet to reach its consensus. The state of the art standard that allows performing spatial and attribute query and manipulation in such environments is the CityGML [83]. Other options under development include the commercial Esri City Engine, combined with analysis tools implemented in ArcGIS. As soon as 3D analysis tools are fully available, it will become interesting to approach the idea of a real 3D solar cadastre, with sophisticated interactive features. In this context, the development of databases that handle 3D geometries, such as Postgis or Oracle, and 3D spatial query languages, e.g. spatial Structured Query Language (SQL), also represent a major challenge. Using SQL, the open source Postgis can be integrated within a GIS environment for visualization through applications such as GLOBE or Horao [100].

In this matter, much effort is still needed to accomplish the creation of a 3D urban model that brings together all issues that the reviewed models can offer. Such tool could represent a key step for the dissemination of BIPV among the general public and to move decision makers to plan cities in order to reach closed to the nZEB goal.

## 6. Conclusions

A review on concepts and models to estimate and represent solar potential in complex landscapes was conducted. After a brief overview of the most relevant empirical models for solar radiation, some of the pioneering software and GIS tools that were introduced to address issues related to the prediction of the solar resource were reviewed. Finally, the most sophisticated and complete models for the urban context were discussed. Solar mapping tools existing on the web were also analysed.

It was shown that the improving ability to describe the physical behaviour of solar radiation has been incorporated into the methods, with model after model trying to overcome previous limitations. The evolution of models has been hand in hand with the development of computer power, as increased computational power is required for more demanding calculations. Thanks to the fast development of information technology, solar mapping models are today far more powerful, allowing user-friendly detailed analysis and representation of the radiation phenomena, thus reaching out outside the traditional architecture and engineering niches. An emerging trend is the employment of these GIS tools for energy analysis in the urban environment.

The major limitations of current models and tools have been highlighted, paving the way for future developments. These include improved data quality, more detailed diffuse radiation and energy conversion modelling, 3D representation and model validation.

## Acknowledgements

This work has been partially supported by MIT Portugal and Portuguese Science Foundation (FCT) Grant: SFRH/BD/52363/2013.

## References

[1] Marszal AJ, Heiselberg P, Bourrelle JS, Musall E, Voss K, Sartori I, et al. Zero Energy Building – a review of definitions and calculation methodologies. Energy Build 2011;43(4):971–9.
[2] Izquierdo S, Rodrigues M, Fueyo N. A method for estimating the geographical distribution of the available roof surface area for large-scale photovoltaic energy-potential evaluations. Sol Energy 2008;82(10):929–39.
[3] Goretzki P. GOSOL – Solarbüro für energieeffiziente Stadtplanung; 2013. [Online]. Available: ⟨http://www.gosol.de/index.html⟩.
[4] Peckham RJ. Shadowpack – P.C. version 2-0 user's guide; 1990.
[5] Rich P, Hetrick W, Saving S. Modeling topographic influences on solar radiation: a manual for the SOLARFLUX Model. Los Alamos, NM; 1995.
[6] Azar S. TownScope; 2013. [Online]. Available: ⟨http://townscope.com/⟩.
[7] Skelion. Skelion 5.0.7 user's guide; 2013.
[8] Ecotect. Autodesk ECOTECT analysis; 2010.
[9] Carneiro C, Morello E, Desthieux G., Golay F. Urban environment quality indicators: application to solar radiation and morphological analysis on built area. In: Advances in visualization, imaging and simulation; 2010. p. 141–8.
[10] Hofierka J, Zlocha M. A new 3-D solar radiation model for 3-D city models. Trans GIS 2012;16(5):681–90.
[11] Jakubiec JA, Reinhart CF. A method for predicting city-wide electricity gains from photovoltaic panels based on LiDAR and GIS data combined with hourly Daysim simulations. Sol Energy 2013;93:127–43.
[12] Catita C, Redweik P, Pereira J, Brito MC. Extending solar potential analysis in buildings to vertical facades. Comput Geosci 2014;66:1–12.
[13] Ramachandra T, Shruthi B. Spatial mapping of renewable energy potential. Renew Sustain Energy Rev 2007;11(7):1460–80.
[14] Koo C, Hong T, Park HS, Yun G. Framework for the analysis of the potential of the rooftop photovoltaic system to achieve the net-zero energy solar buildings. Prog Photovol: Res Appl 2013;22:462–78.
[15] Angelis-Dimakis A, Biberacher M, Dominguez J, Fiorese G, Gadocha S, Gnansounou E, et al. Methods and tools to evaluate the availability of renewable energy sources. Renew Sustain Energy Rev 2011;15(2):1182–200.
[16] Duffie JA, Beckman WA. Solar engineering of thermal processes. Hoboken, NJ, USA: John Wiley & Sons, Inc.; 2013.
[17] Chwieduk DA. Recommendation on modelling of solar energy incident on a building envelope. Renew Energy 2009;34(3):736–41.
[18] Liu BY H, Jordan RC. The interrelationship and characteristic distribution of direct, diffuse and total solar radiation. Sol Energy 1960;4(3):1–19.
[19] Hay JE. Calculation of monthly mean solar radiation for horizontal and inclined surfaces. Sol Energy 1979;23(4):301–7.
[20] Perez R, Seals R, Ineichen P, Stewart R, Menicucci D. A new simplified version of the perez diffuse irradiance model for tilted surfaces. Sol Energy 1987;39(3):221–31.
[21] Noorian AM, Moradi I, Kamali GA. Evaluation of 12 models to estimate hourly diffuse irradiation on inclined surfaces. Renew Energy 2008;33(6):1406–12.
[22] Perez R, Stewart R, Arbogast C, Seals R, Scott J. An anisotropic hourly diffuse radiation model for sloping surfaces: description, performance validation, site dependency evaluation. Sol Energy 1986;36(6):481–97.
[23] Perez R, Ineichen P, Seals R, Michalsky J, Stewart R. Modeling daylight availability and irradiance components from direct and global irradiance. Sol Energy 1990;44(5):271–89.
[24] Mondol JD, Yohanis YG, Norton B. Solar radiation modelling for the simulation of photovoltaic systems. Renew Energy 2008;33(5):1109–20.
[25] Evseev EG, Kudish AI. The assessment of different models to predict the global solar radiation on a surface tilted to the south. Sol Energy 2009;83(3):377–88.

[26] Ma CC Y, Iqbal M. Statistical comparison of models for estimating solar radiation on inclined surgaces. Sol Energy 1983;31(3):313–7.
[27] Muneer T. *Solar radiation and daylight models*. Oxford, UK: Elsevier Butterworth-Heinemann; 2004; 345.
[28] Gueymard CA. Direct and indirect uncertainties in the prediction of tilted irradiance for solar engineering applications. Sol Energy 2009;83(3):432–44.
[29] Reindl DT, Beckman WA, Duffie JA. Evaluation of hourly tilted surface radiation models. Sol Energy 1990;45(1):9–17.
[30] Skartveit A, Olseth J Asle. Modelling slope irradiance at high latitudes. Sol Energy 1986;36(4):333–44.
[31] Gueymard C. An anisotropic solar irradiance model for tilted surfaces and its comparison with selected engineering algorithms. Sol Energy 1987;38 (5):367–86.
[32] Grigiante M, Mottes F, Zardi D, de Franceschi M. Experimental solar radiation measurements and their effectiveness in setting up a real-sky irradiance model. Renew Energy 2011;36(1):1–8.
[33] Bird RE, Hulstrom RL. A simplified clear sky model for direct and diffuse insolation on horizontal surfaces, Colorado; 1981.
[34] Perez R, Seals R, Stewart R. Assessing the load matching capability of photovoltaics for US utilities based upon satellite-derived insolation data. In: Conference record of the twenty third IEEE photovoltaic specialists conference – 1993 (cat. no.93CH3283-9); 1993. p. 1146–51.
[35] Magarreiro C, Brito MC, Soares PMM. Assessment of diffuse radiation models for cloudy atmospheric conditions in the Azores region. Sol Energy 2014;108:538–47.
[36] Ivanova SM. Estimation of background diffuse irradiance on orthogonal surfaces under partially obstructed anisotropic sky. Part I – Vertical surfaces. Sol Energy 2013;95:376–91.
[37] Ivanova SM. Estimation of background diffuse irradiance on orthogonal surfaces under partially obstructed anisotropic sky. Part II – horizontal surfaces. Sol Energy 2014;100:234–50.
[38] Dubayah R. Estimating net solar radiation using Landsat Thematic Mapper and digital elevation data. Water Resour Res 1992;28(9):2469–84.
[39] Dubayah R, Rich PM. Topographic solar radiation models for GIS. Int J Geograph Inf Syst 1995;9(4):405–19.
[40] Tregenza PR. Subdivision of the sky hemisphere for luminance measurements. Light Res Technol 1987;19(1):13–4.
[41] Marsh AJ. Sky subdivision. Natural Frequency; 2011. [Online]. Available: ⟨http://naturalfrequency.com/wiki/sky-subdivision⟩.
[42] Littlefair P. Passive solar urban design : ensuring the penetration of solar energy into the city. Renew Sustain Energy Rev 1998;2(3):303–26.
[43] Rakovec J, Zakšek K. On the proper analytical expression for the sky-view factor and the diffuse irradiation of a slope for an isotropic sky. Renew Energy 2012;37(1):440–4.
[44] Redweik P, Catita C, Brito M. Solar energy potential on roofs and facades in an urban landscape. Sol Energy 2013;97:332–41.
[45] Ratti C, Richens P. Raster analysis of urban form. Environ Plan B: Plan Des 2004;31(2):297–309.
[46] Mészároš I, Miklánek P, Parajka J. Solar energy income modelling in mountainous areas. ERB and Northern European FRIEND Project 5 Conference; 2002.
[47] Hetrick W, Rich P, Weiss S. Modeling insolation on complex surfaces. In: Proceedings of the thirteenth annual ESRI user conference, vol. 2; 1993. p. 447–58.
[48] Rich P, Hetrick W, Saving S. Modeling topographic influences on solar radiation: a manual for the SOLARFLUX model; 1995.
[49] Kumar L, Skidmore AK, Knowles E. Modelling topographic variation in solar radiation in a GIS environment. Int J Geograph Inf Sci 1997;11(5):475–97.
[50] Ward GJ. The RADIANCE lighting simulation and rendering system. In: Proceedings of the 21st annual conference on Computer graphics and interactive techniques – SIGGRAPH '94; 1994. p. 459–72.
[51] Compagnon R. Solar and daylight availability in the urban fabric. Energy Build 2004;36(4):321–8.
[52] Robinson D. Urban morphology and indicators of radiation availability. Sol Energy 2006;80(12):1643–8.
[53] Jakubiec J, Reinhart C. DIVA 2.0: integrating daylight and thermal simulations using Rhinoceros 3D, Daysim and EnergyPlus. In: 12th conference of international Building Performance Simulation Association; 2011. p. 14–6.
[54] Robinson D, Stone A. Irradiation modelling made simple: the cumulative sky approach and its applications. In: Proceedings of PLEA conference, September 2004; p. 19–22.
[55] Perez R, Seals R, Michalsky J. To all-weather model for sky luminance distribution—preliminary configuration and validation. Sol Energy 1993;51(5):423.
[56] Mardaljevic J. Simulation of annual daylighting profiles for internal illuminance. Light Res Technol 2000;32(3):111–8.
[57] Reinhart C. Daysim; 2013. [Online]. Available: ⟨http://daysim.ning.com/⟩.
[58] Fu P, Rich P. Design and implementation of the Solar Analyst: an ArcView extension for modeling solar radiation at landscape scales. In: Proceedings of the 19th annual ESRI user conference; 1999.
[59] Wiginton LK, Nguyen HT, Pearce JM. Quantifying rooftop solar photovoltaic potential for regional renewable energy policy. Comput Environ Urban Syst 2010;34(4):345–57.
[60] Faessler J. Evaluation du potentiel solaire en milieu urbain : essais d'application aux toitures du canton de Genève; 2010.
[61] Mendes M. Localização e caracterização de locais com potencial para produção de energia solar-Caso de estudo no nordeste de Portugal; 2010.
[62] Brito MC, Gomes N, Santos T, Tenedório J a. Photovoltaic potential in a Lisbon suburb using LiDAR data. Sol Energy 2012;86(1):283–8.
[63] Wilson JP, Gallant JC. Secondary topographic attributes. *Terrain analysis. Principles and applications*. New York: John Wiley & Sons, Inc.; 2000; 87–132.
[64] Knowles RL. The solar envelope: its meaning for energy and buildings. Energy Build 2003;35(1):15–25.
[65] Pereira FO R, Silva CA N, Turkienikz B. A methodology for sunlight urban planning: a computer-based solar and sky vault obstruction analysis. Sol Energy 2001;70(3):217–26.
[66] Ratti C, Morello E. SunScapes: extending the 'solar envelopes' concept through 'iso-solar surfaces.' In: Proceedings of PLEA2005 – The 22nd international conference on Passive and Low Energy Architecture; 2005.
[67] Chimklai P, Hagishima A, Tanimoto J. A computer system to support Albedo Calculation in urban areas. Build Environ 2004;39(10):1213–21.
[68] Rigollier C, Bauer O, Wald L. On the clear sky model of the ESRA—European Solar Radiation Atlas—with respect to the Heliosat method. Sol energy 2000;68(1):33–48.
[69] Beyer HG, Costanzo C, Heinemann D. Modifications of the Heliosat procedure for irradiance estimates from satellite images. Sol Energy 1996;56 (3):207–12.
[70] Hofierka J. Direct solar radiation modelling within an open GIS environment. In: Geogr. Inf. '97 From Res. to Appl. through Coop. vols. 1, 2; 1997; Proceedings of JEC-GI'97 conference in Vienna, Austria, IOS Press Amsterdam, 575-584.
[71] Hofierka J, Suri M. The solar radiation model for Open source GIS: implementation and applications. In: Open source GIS – GRASS users conference; September 2002; p. 11–3.
[72] Šúri M, Huld T a, Dunlop ED. PV-GIS: a web-based solar radiation database for the calculation of PV potential in Europe. Int J Sustain Energy 2005;24 (2):55–67.
[73] Hofierka J, Kaňuk J. Assessment of photovoltaic potential in urban areas using open-source solar radiation tools. Renew Energy 2009;34(no. 0):2206–14.
[74] Matzarakis A, Rutz F, Mayer H. Modelling radiation fluxes in simple and complex environments: basics of the RayMan model. Int J Biometeorol 2010;54(2):131–9.
[75] Pereira F, Leder S, Moraes L, Lenzi C. Sky obstruction and daylight. In: Proceedings of PLEA2009–26th conference on Passive and Low Energy Architecture, June 2009; p. 22–4.
[76] Tooke TR, Coops NC, Christen A, Gurtuna O, Prévot A. Integrated irradiance modelling in the urban environment based on remotely sensed data. Sol Energy 2012;86(10):2923–34.
[77] Melo EG, Almeida MP, Zilles R, Grimoni J a B. Using a shading matrix to estimate the shading factor and the irradiation in a three-dimensional model of a receiving surface in an urban environment. Sol Energy 2013;92:15–25.
[78] Erdélyi R, Wang Y, Guo W, Hanna E, Colantuono G. Three-dimensional SOlar RAdiation Model (SORAM) and its application to 3-D urban planning. Sol Energy 2014;101:63–73.
[79] Ruiz-Arias JA, Tovar-Pescador J, Pozo-Vázquez D, Alsamamra H. A comparative analysis of DEM-based models to estimate the solar radiation in mountainous terrain. Int J Geograph Inf Sci 2009;23(8):1049–76.
[80] Jochem A, Höfle B, Rutzinger M, Pfeifer N. Automatic roof plane detection and analysis in airborne lidar point clouds for solar potential assessment. Sensors 2009;9(7):5241–62.
[81] Redweik P, Catita C, Brito MC. 3D local scale solar radiation model based on urban LiDAR data. In: Proceedings of ISPRS; 2011.
[82] Jochem A, Höfle B, Rutzinger M. Extraction of vertical walls from mobile laser scanning data for solar potential assessment. Remote Sens 2011;3 (12):650–67.
[83] Nouvel R, Schulte C., Eicker U, Pietruschka D, Coors V. CityGML-based 3D city model for energy diagnostics and urban energy policy support. In: Proceedings of the 13th conference of international Building Performance Simulation Association, 2013; p. 218–25.
[84] Teller J, Azar S. Townscope II—a computer system to support solar access decision-making. Sol Energy 2001;70(3):187–200.
[85] Miguet F, Groleau D. Simulation tool including transmitted direct and diffuse light: application to the evaluation of daylighting inside glazed intermediate spaces. In: Proceedings of the 7th IBPSA; 2001. p. 907–14.
[86] Ho LJ, Mestayer P, Henon A. 3D simulation of thermal signatures in the urban canopy layer by using the thermo-radiative model SOLENE ide.titech.ac.jp, July 2009; p. 1–4.
[87] Groleau D, Fragnaud F, Rosant J. Simulation of the Radiative Behaviour of an Urban Quarter of Marseille with the SOLENE Model'. In: Proceedings of ICUC5, Fifth International Conference on Urban Climate; 2003.
[88] Vangimalla PR, Olbina SJ, Issa RR, Hinze J. Validation of Autodesk Ecotect™ accuracy for thermal and daylighting simulations. In: Proceedings of the 2011 Winter Simulation Conference (WSC); 2011. p. 3383–94.
[89] Abdul-Rahman A, Pilouk M. *Spatial data modelling for 3D GIS*. Berlin, Heidelberg: Springer; 2008; 302.
[90] Dean J, Kandt A, Burman K. Analysis of web-based solar photovoltaic mapping tools. In: ASME 3rd conference on energy sustainability; 2009.
[91] Huld T, Suri M, Kenny RP, Dunlop ED. Estimating PV performance over large geographical regions. In: Conference record of the thirty-first ieee photovoltaic specialists conference, January 2005; p. 1679–82.
[92] Huld T, Müller R, Gambardella A. A new solar radiation database for estimating PV performance in Europe and Africa. Sol Energy 2012;86 (6):1803–15.

[93] Marion B, Anderberg M, George R. PVWATTS version 2—enhanced spatial resolution for calculating grid-connected PV performance. In: NCPV program review meeting; October 2001. p. 0–3.
[94] IMBY. In My Backyard; 2013. [Online]. Available: ⟨http://www.nrel.gov/eis/imby/⟩.
[95] Suri M, Huld T, Cebecauer T, Dunlop ED. Geographic aspects of photovoltaics in Europe: cContribution of the PVGIS Website. IEEE J Sel Top Appl Earth Obs Remote Sens 2008;1(1):34–41.
[96] Redweik P, Catita C, Brito MC. PV Potential estimation using 3D local scale solar radiation model based on urban LIDAR data. In: 26th European photovoltaic solar energy conference; 2011. p. 3–5.
[97] Loïc Q. Evaluation du potentiel solaire photovoltaique et thermique dans un environnement urbain. Université de Genève; 2012.
[98] Nault É, Rey E, Andersen M. "Early design phase evaluation of urban solar potential: insights from the analysis of six projects," in 13th Conference of International Building Performance Simulation Association, 2013, pp. 177–184.
[99] Zlatanova S. On 3D topological relationships. In: Proceedings 11th international workshop on database and expert systems applications; 2000. p. 913–9.
[100] Oslandia. OslandiaTechnos; 2014. [Online]. Available: ⟨http://www.oslandia.com/pages/technos.html⟩.